

## **Ultrasound Propagation Velocity in Porcine Trabecular Vertebral Bone Following Single-Dose Stereotactic Radio Surgery**

**Julie P. Griffin**

Department of Mechanical Engineering  
Southern Methodist University  
3101 Dyer Street  
Dallas, Texas 75205  
USA

**Paul M. Medin**

Department of Radiation Oncology  
University of Texas - Southwestern Medical Center at Dallas  
5323 Harry Hines Boulevard  
Dallas, Texas 75390  
USA

**Edmond Richer**

Department of Mechanical Engineering  
Southern Methodist University  
3101 Dyer Street  
Dallas, Texas 75205  
USA

### **Abstract**

*Recently, there has been a move towards single-fraction SRS treatments with doses as great as 24 Gy. This increase has resulted in concerns due to the increased rates of late onset vertebral fractures, possibly indicating that the maximum tolerance to radiation has been exceeded. The long-term effect of SRS on the structural integrity of bone is still unknown. This study uses Ultrasound Propagation Velocity (UPV), predictive of mechanical strength, as an indicator for changes in bone properties. SRS was administered to four Yucatan minipigs at 16 - 18 Gy from the fourth to the sixth cervical vertebrae, focused on half the vertebral body in the medial-lateral direction. The UPV was found to be statically different between the halves of irradiated vertebrae, absent in the non-irradiated vertebrae. These results infer that current accepted doses for single-fraction SRS do cause changes in the mechanical properties of bone.*

**Keywords:** Ultrasound Propagation Velocity, Spinal SRS

### **1. Introduction**

Each year, more than 100,000 individuals in the United States are affected by vertebral metastases from breast, lung, prostate, myeloma, and renal malignancies (Black, 1979; Byrne & Waxman, 1990). The most common side effects of growing vertebral tumors include the loss of sensory and motor skills, debilitating pain, and vertebral collapse. A combination of external beam radiation therapy and steroids has proven effective for palliation of skeletal metastases, providing pain relief with minimal morbidity.

Stereotactic Radiosurgery (SRS) is an image-guided outpatient procedure that facilitates the accurate delivery of high dose radiation while the surrounding tissue is relatively spared. Many investigators have pursued the use of SRS at single-fraction doses above eight Gray (Gy) to treat spinal metastases. Approximately 90% of patients showed durable pain reduction and 80% or greater experienced high rates of local control (Gerszten, et al., 2007; Yamada, et al., 2008). The improved control of cancer at the origin site combined with surgery and radiation is credited for the increased survival in patients with spinal cord compression from metastasis (Jemal, et al., 2008; Patchell, et al., 2005).

In breast and lung irradiation, the close proximity of bones to the targeted cancer results in unavoidable exposure. Nevertheless, the bone tissue receives a minimal dose of radiation. Conversely, when spinal SRS is used to manage bone metastases, vertebrae are intentionally irradiated with large doses. In lung irradiation at 24 - 37 Gy in 1 - 5 fractions (Fritz, et al., 2008; Zimmermann, et al., 2005) a larger percentage of fractures has been observed compared to historical clinical data (Parker & Berry, 1975). As clinical experience with spinal SRS has been acquired, prescription doses have increased from 12 Gy up to doses as large as 24 Gy. One group of researchers observed an unusually high vertebral fracture rate of approximately 39% following 24 Gy treatments (Rose, et al., 2009; Yamada, et al., 2008).

The long-term effects of high dose irradiation on bone are not well known. Dose escalation may have exceeded the vertebral body's ability to preserve their structural integrity. Rissanen (1969b, 1969a) and his fellow researchers reported the short-term effect of single-dose radiation (from 5 Gy to 40 Gy) on the bone turnover in dogs for the humerus, femur, and patella (Rokkanen, Rissanen, & Paastama, 1969). After four days, bone spaces had poor cellularity at five Gy, new mineralized areas occurred in the cancellous spaces at 10 Gy and osteocytes were radioresistant up to 40 Gy. The two-week assessment showed similar results in addition to the cancellous spaces were acellular and the bone had become partly anuclear. It was also noted at 40 Gy, the density of the trabecular bone had appeared to decrease. Although new bone formation was observed at the two-month evaluation, the trabeculae were thin, acellular and displayed fragmentation in some areas. The cancellous spaces were either empty or contained fatty tissue. Thrombosed blood vessels were observed in the groups who received 10 Gy and 40 Gy. Due to the short time period of this study, it is unknown if the blood vessels continued to harden or if new bone formed. The sensitivity of bone marrow to radiation has been extensively researched, showing that even low doses of radiation deplete the bone marrow's ability to form new blood cells. In addition, fatty marrow replacement was observed long term (Hall, et al., 1988; Mell, et al., 2008). With the increasing use of large dose fractions in radiation therapy, an accurate, non-invasive method to evaluate the biomechanical properties of bone would allow future studies to determine the long-term sequelae of irradiation in patients.

Ultrasound is a technique that offers significant advantages over mechanical methods for testing the bone properties, including: non-destructive nature, cost efficiency, and ability to be used in a non-invasive way with patients. The Ultrasound Propagation Velocity (UPV) in solids is deterministically related to the mechanical stiffness (elastic modulus) of the material, a relationship that has been experimentally validated for bone (An & Draughn, 2000; Cavani, et al., 2008; Gluer, 2007; Hans, et al., 1995; Mehta, et al., 2001). In contrast to other materials, bone material elastic modulus and ultimate strength are statically related (Abendschein & Hyatt, 1970; Antich, et al., 1991; Rho, Ashman, & Turner, 1993). Thus, non-invasive approaches based on ultrasound have been proposed to assess bone strength by measuring the UPV both *in vitro* (Antich, et al., 1991; Mehta, et al., 2001) and *in vivo* (Richer, et al., 2005).

In this study, the cervical vertebrae of four adolescent Yucatan minipigs were partially irradiated at current accepted doses with spinal SRS. After one year, the UPV from irradiated and non-irradiated vertebrae samples were compared, using the Short-Time Fourier Transform (STFT) method. The purpose of this study was to assess the use of UPV as an indicator of SRS effect on the biomechanical properties of bone.

## **2. Materials and Methods**

### **2.1 Animal Model and Sample Preparation**

Although humans and quadrupeds differ in the orientation of the spinal column, the axial compression of a quadruped created by its musculature is similar to the axial compression in the human spine due to the vertical posture and gravity (Smit, Odgaard, & Schneider, 1997; Smit T. H., 2002). Thus, both have vertebra whose bone microstructure is oriented from end-plate to end-plate. Adolescent Yucatan minipigs were used as the biological model due to the identical number and similar size of the pig cervical vertebrae to the human cervical vertebrae. Additionally, humans and pigs have comparable physiological functions such as the gastrointestinal system, blood supply, mechanical characteristics of the spine, and bone remodeling (Busscher, et al., 2010; Reinwald & Burr, 2008; Smith, 2000).

Four adolescent Yucatan minipigs received spinal Stereotactic Radio Surgery (SRS) (*Novalis* Linear Accelerator BrainLAB AG, Feldkirchen, Germany) from the fourth to the sixth cervical vertebrae, focusing on the left half of the vertebral body in the medial-lateral direction (Medin, et al., 2011).

The radiation was focused parallel to the cervical spinal cord crating a cylindrical dose volume about 2 cm in diameter and 5 cm in length. A steep dose gradient was created across the vertebral bodies (see Fig. 1 for the 90%, 50% and 10% isodose lines). Animals A and B received 16 Gy to the 90% isodose line, while animals C and D received 18 Gy to the 90% isodose line (see Table 1). On average, for an irradiated vertebra, the left side (high dose side) received 16 – 18 Gy and the right side (low dose side) received 6 – 8 Gy. For a minimum of 12 months, the locomotion abilities of the four animals were observed at the University of Texas Southwestern Medical Center at Dallas (UTSWMC) to determine the effects of radiation on the spinal cord. After the 12-month period, the animals were euthanized (Medin, et al., 2011). The cervical vertebrae were removed and imaged using micro x-ray Computed Tomography ( $\mu$ CT). The vertebrae were kept in a 0.9% saline solution. This study was approved by the institutional Animal Care and Use Committee at the UTSWMC and conformed to all national and local regulations regarding the use of animals for research.

One irradiated and one non-irradiated vertebra from each animal was selected for analysis as detailed in Table 1. The cervical vertebral bodies were cut using a low speed bone saw (Buehler Isomet Low Speed, Lake Bluff, IL, USA) into two  $5 \times 6 \times 7 \text{ mm}^3$  rectangular cuboid of trabecular bone, separating the left and right sides symmetric about the center of the vertebra. Each vertebra was cut using the same procedure, creating the same alignment relevant to the anatomical direction of the animal, allowing for easy directional identification (the 7 mm length corresponds to the rostral-caudal, 6 mm length aligns to the dorsal-ventral, and 5 mm to the lateral-medial directions respectively). Thus, for each animal four different samples of bone were examined: (1) irradiated left side, (2) irradiated right side, (3) non-irradiated left side, and (4) non-irradiated right side as seen in Fig. 2.

The trabecular samples were stored in individual acrylic containers filled with a 0.9% saline solution at  $-30^\circ\text{C}$  (Laursen, et al., 2003). The bone marrow was not removed in order to keep the bones as close to their original *in vivo* state as possible. The dimensions of each trabecular bone sample were measured using a digital caliper, and mass and density were determined prior to the ultrasound study.

## 2.2 Experimental Setup and Measurement Procedure

Bone is a living component of the body that evolves throughout life due to varying internal and external factors such as aging, fractures, or receiving radiation treatment (Laguier & Haïat, 2011). Traditionally, ultrasound measurements in trabecular bone have been conducted on relatively large bone samples at low frequency, several kilohertz, such that the wavelength is larger than the characteristic dimensions of the bone structure but smaller than the overall sample size (An & Draughn, 2000; Nicholson, 2008; Renaud, et al., 2008). Conversely, in this study, the trabecular bone samples obtained from the porcine vertebrae were small relative to the bone specimens used in other reported research. In order to ensure the most accurate measurement of the UPV for the given sample size, a frequency of 1 MHz was selected as detailed in Pollard (2009) and Pollard, et al., (2011).

A pair of matched frequency (1MHz) ultrasound transducers (A303s, Olympus NDT Inc., Waltham, MA, USA) was arranged in a through-transmission configuration along the rostral-caudal direction of the bone sample as seen in Fig. 3. An acrylic cap was used to position the bone sample outside the near field of the emitter (bottom transducer). Room temperature water for the bottom transducer and ultrasound gel for the top transducer were used as coupling agents. An ultrasonic pulser-receiver (model 5072PR, Olympus NDT Inc., Waltham, MA, USA) was used to generate a high voltage, narrow pulse (200V, 25ns) to excite the transducers. The received signal was amplified using the pulser-receiver amplifier with a gain selected to optimize the signal-to-noise (S/N) ratio. A high-speed digitizer (NI Scope Card USB-5133, National Instruments, Austin, TX) sampled the signal at a rate of 100 MS/s with 12-bit resolution. Custom software written in LabVIEWv8.2 (National Instruments, Austin, TX, USA) was used to display and record the output ultrasound signal. In order to reduce the noise, the signal was averaged for 10 s before storage and each measurement was repeated five times. The digitized ultrasound signal for each sample was imported into a custom analysis software using Igor Pro 6.03A (WaveMetrics, Inc., Lake Oswego, OR, USA) programming environment. A typical ultrasound signal through a trabecular vertebral bone sample is presented in Fig. 4.

Unlike velocity calculations based on time-of-flight (TOF), the Short-Time Fourier Transform method allows for the determination of arrival time of mono-frequency components extracted from the transmitted ultrasound pulse at a pre-determined position in space (Zhao, Basir, & Mittal, 2005). Traditionally STFT has been used to determine ultrasound dispersion and attenuation through non-porous materials.

The STFT of a signal  $s(t)$  is defined as

$$G_{\phi_s}(b, \omega) = \int_{-\infty}^{\infty} s(t)\phi_{\omega}(t - b)e^{-j\omega t} dt$$

where  $\omega$  is the angular frequency and  $\phi_{\omega}(t)$  is a windowing function

$$\phi_{\omega}(t) = \begin{cases} \phi(t), & t \in [b - \tau, b + \tau] \\ 0, & \text{otherwise} \end{cases}$$

Where  $b$  is the moment in time,  $\tau > T$  is the time window width,  $T$  is the period of the wave, and  $j = \sqrt{-1}$ . A Hanning Window function was chosen as the windowing function,  $\phi(t)$ , for its smoothing properties (see Fig. 4, dashed line). In essence, sliding the window function by changing the specified moment in time,  $b$ , the STFT calculates the amplitude distribution of Fourier transform, indicative of wave energy, for a selected frequency component along the temporal axis (Fig. 5). The STFT amplitude reaches maximum when the signal passes through the receiver location.

The ultrasound propagation time,  $t$ , was obtained from the time coordinate of the first peak in the STFT time plot. The propagation time obtained by STFT with the receiver in direct contact with the transmitter's acrylic cap,  $t_o$ , was used as reference, and the UPV,  $v$ , was calculated as,

$$v = \frac{L_{rc}}{t - t_o}$$

where  $L_{rc}$  is the bone sample length in the rostral-caudal direction.

### 3. Results

Observations about the physical appearance of the vertebrae were made before extraction of the samples. As seen in Fig. 6, the irradiated vertebrae have observable asymmetry between the high dose radiation side (left side) and the low dose side (right side). In addition to the transverse process being noticeably smaller on the left side, it was generally observed that the irradiated sides of the vertebral bodies were shorter in the rostral-caudal direction. While some vertebrae only displayed slight asymmetry, other cases were more extreme, with transverse processes missing entirely (Fig. 7).

The calculated average and standard deviation values for the UPV are listed in Table 2. Due to the limited dosage values in this study, determining if a linear relationship between the administered dose and UPV exists was not feasible.

It is seen that  $t$ -test1a compares the left side of the non-irradiated vertebra to the right side of the non-irradiated vertebrae, while  $t$ -test1b compares the left side to the right side of the irradiated vertebra. In  $t$ -tests1a and 1b, the side of the vertebra that was not targeted for radiation (right side) served as control for the side that was the irradiated (left side). As summarized in Table 2, the  $p$ -value for  $t$ -test1a indicates that the UPV are the same ( $p = 0.8196$ ), whereas the  $p$ -value for  $t$ -test1b indicates that the UPV are not the same ( $p = 0.0095$ ).

The additional two  $t$ -tests,  $t$ -test2a and 2b compared each side of the non-irradiated vertebrae to the same side of the irradiated vertebrae. The results for both  $t$ -tests,  $p = 0.0129$  and  $p = 0.0386$  respectively, imply that there is a difference in UPV between two vertebra for both the right and left sides (Fig. 9).

### 4. Discussion

This experimental study examined the effect of single-dose SRS applied to a selected volume within the cervical vertebrae of four adolescent Yucatan minipigs, at radiation dosages that are currently used in clinical practice for palliative treatment of spinal metastases. The treatment plan was designed to expose selectively the C4 - C6 vertebrae to a dose gradient. One year after irradiation, the animals were euthanized and the cervical spines were removed and inspected for gross anomalies.

It was generally observed that the irradiated side of the vertebral bodies was shorter in the rostral-caudal direction and the transversal processes were shorter and thinner, creating overall spine asymmetry. In one case, the transverse process on the irradiated side was completely atrophied. These observations suggest that in the long term, SRS severely affected the bone remodeling and growth.

Two trabecular bone samples, symmetrically located in the lateral-medial direction, were obtained from one irradiated and one non-irradiated vertebrae from each animal. The UPV determined by STFT was measured through the trabecular bone samples in the rostral-caudal direction.

The STFT method provided accurate UPV measurements, as seen by the low values for the standard deviation. The average UPV values for all animals for the sample obtained from the left side of the irradiated vertebrae ( $2,416.83 \pm 25.91$  m/s), which received the high dose treatment, was consistently lower than the UPV average for the right side sample ( $2,518.28 \pm 24.90$  m/s). This difference represents a 4% reduction and was statistically significant as shown by the *t*-test1b ( $p = 0.0095$ ). In contrast, the non-irradiated vertebrae average UPV for the left and right sides were statistically the same (*t*-test1a,  $p = 0.8196$ ). These results suggest that the SRS caused a change in the irradiated vertebrae tissue, as shown by the UPV. Based on the well-documented relationship between UPV and bone tissue mechanical properties, it can be inferred that the strength of the vertebrae was affected.

The UPV for the same sides of irradiated and non-irradiated vertebrae were deemed different by the results of *t*-test2a ( $p = 0.0129$ ) and *t*-test2b ( $p = 0.0386$ ) for the right and left sides respectively. Since the right side of the irradiated vertebrae received in average a dose of 6 – 8 Gy, the result would seem to indicate that even the low dose irradiation produced a significant change in material properties. Nevertheless, a more careful analysis reveals that there are large differences in the UPV between vertebrae. For example, the average UPV for the two non-irradiated vertebrae employed in the study (C3 and C7) were  $2,183.06 \pm 39.53$  m/s and  $2,500.78 \pm 35.19$  m/s respectively and a *t*-test comparison showed significance ( $p = 1.27 \times 10^{-8}$ ). This suggests that the UPV differs significantly between vertebrae regardless of exposure to radiation, most likely due to different anatomical and mechanical load requirements. As a result, direct comparison between the UPV values obtained for different vertebrae could be problematic.

Inconsistency in the selection of the non-irradiated and irradiated vertebrae across different animals is a potential weakness of this study. Thus, the most reliable results are those that compare the UPV values for the adjacent sides of the same vertebra.

## 5. Conclusions

Although single-fraction SRS treatment for skeletal metastases is being increasingly used in clinical oncology, the long-term effects of high-dose irradiation on bone tissue are still unknown. Doses of 16 - 18 Gy are commonly prescribed in clinical practice and larger doses have been reported with increased fracture rates. In this study, the Ultrasound Propagation Velocity was used as an indicator for changes in the mechanical properties of bone tissue due to radiation. A statistically significant 4% lower UPV was measured in the side of the irradiated vertebrae, one year after single-fraction SRS, compared to the adjacent side that received a much lower dose. Based on the well-documented relationship between UPV and the mechanical properties of trabecular bone tissue, it can be inferred that SRS caused a change in mechanical properties in the irradiated bone tissue. Most importantly, it is suggested that the current accepted doses of SRS do cause a long-term change in the mechanical properties of cervical vertebra bone, as shown by the UPV.

In the future, a comparison of UPV values before and after radiation therapy may be a useful metric of bone health. UPV would be a good indicator to determine if a detrimental effect was produced by SRS and provide guidelines for follow-up treatment. As found in this study, blindly comparing the UPV for different vertebrae is not recommended since their UPV, and mechanical properties, may differ due to adaptation to different mechanical loads and anatomical functionality.

## Acknowledgements

This work was partially supported by NIH R01-049517 grant, and by a startup grant from Bobby B. Lyle School of Engineering, SMU, Dallas, TX, USA.

## References

- Abendschein, W., & Hyatt, G. (1970). Ultrasonics and related physical properties of bone. *Clinical Orthopaedics and Related Research*, 69, 294-301.
- An, Y. H., & Draughn, R. A. (2000). *Mechanical Testing of Bone and the Bone – Implant Interface*. Boca Raton: CRC Press.
- Antich, P. P., Anderson, J. A., Ashman, R. B., Dowdey, J. E., Gonzales, J., Murry, R. C., et al. (1991). Measurement of mechanical properties of bone material in vitro by ultrasound reflection: Methodology and comparison with ultrasound transmission. *Journal of Bone and Mineral Research*, 6, 417-426.
- Black, P. (1979, Dec). Spinal metastasis: current status and recommended guidelines for management. *Neurosurgery*, 5(6), 726-746.
- Busscher, I., Ploegmakers, J., Verkerke, G., & Veldhuizen, A. (2010). Comparative anatomical dimensions of the complete human and porcine spine. *Eurospine Journal*, 19, 1104-1114.
- Byrne, T. N., & Waxman, S. G. (1990). *Spinal Cord Compression: Diagnosis And Principles Of Management (Contemporary Neurology Series)*. Philadelphia: F.A. Davis.
- Cavani, F., Giavaresi, G., Fini, M., Bertoni, L., de Terlizzi, F., Barkmann, R., et al. (2008, July). Influence of Density, Elasticity, and Structure on Ultrasound Transmission Through trabecular Bone Cylinders. *IEEE Transactions on Ultrasonics, Ferroelectrics, and Frequency Control*, 55(7), 1495-1472.
- Fritz, P., Kraus, H.-J., Blaschke, T., Muehlnickel, W., Strauch, K., Engel-Riedel, W., et al. (2008). Stereotactic, high single-dose irradiation of stage I non-small cell lung cancer (NSCLC) using four-dimensional CT scans for treatment planning. *Lung Cancer*, 60, 193-199.
- Gerszten, P. C., Burton, S. A., Ozhasoglu, C., & Welch, W. C. (2007). Radiosurgery for Spinal Metastases: Clinical Experience in 500 Cases From a Single Institution. *Spine*, 32, 193-199.
- Gluer, C. C. (2007). Quantitative ultrasound-It is time to focus research efforts. *Bone*, 40, 9-13.
- Hall, E., Marchese, M., Hei, T., & Zaider, M. (1988). Radiation response characteristics of human cells in vitro. *Radiation Research*, 114(3), 415-424.
- Hans, D., Arlot, M., Schott, A., Roux, J., Kotzki, P., & Meunier, P. (1995). Do ultrasound measurements on the *os calcis* reflect more the bone microarchitecture than the bone mass?: A two-dimensional histomorphometric study. *Bone*, 16(3), 295 - 300.
- Jemal, A., Siegel, R., Ward, E., Hao, Y., Xu, J., & Murray, T. (2008). Cancer statistics. *Cancer Journal for Clinicians*, 5(2), 71-96.
- Laguier, P., & Haiat, G. (2011). *Bone Quantative Ultrasound*. Dordrecht: Springer.
- Laursen, M., Christensen, F. B., Bungler, C., & Lind, M. (2003, August). Optimal handling of fresh cancellous bone graft: different peroperative storing techniques evaluated by an in vitro osteoblast-like cell metabolism. *Acta orthopaedica Scandinavica*, 74(4), 490-496.
- Medin, P. M., Foster, R. D., van der Kogel, A. J., Sayre, J., McBride, W. H., & Solberg, T. D. (2011). Spinal cord tolerance to single-fraction partial-volume irradiation: a swine model. *International Journal of Radiation Oncology, Biology, Physics*, 79(1), 226-232.
- Mehta, S. S., Antich, P. P., Daphtary, M. M., Bronson, D. G., & Richer, E. (2001). Bone Material Ultrasound Velocity is Predictive of Whole Bone Strength. *Ultrasound in Medicine and Biology*, 27(6), 861-867.
- Mell, L. K., Tiryaki, H., Ahn, K. H., Mundt, A. J., Roeske, J. C., & Aydogan, B. (2008). Dosimetric comparison of bone marrow-sparing intensity-modulated radiotherapy versus conventional techniques for treatment of cervical cancer. *International Journal of Radiation Oncology Biology Physics*, 71(5), 1504-1510.
- Nicholson, P. H. (2008, July). Ultrasound and the Biomechanical Competence of Bone. *IEEE Transactions on Ultrasonics, Ferroelectrics, and Frequency Control*, 55(7), 1539-1545.
- Parker, R. G., & Berry, H. C. (1976). Late effects of therapeutic irradiation on the skeleton and bone marrow. *Cancer*, 37(2), 1162-1171.
- Patchell, R. A., Tibbs, P. A., Regine, W. F., Payne, R., Saris, S., Kryscio, R. J., et al. (2005). Direct decompressive surgical resection in the treatment of spinal cord compression caused by metastatic cancer: a randomised trial. *Lancet*, 366, 643-648.
- Pollard, J. E. (2009). *The Optimization of Ultrasound Measurement Methodology for the Detection of the Effect of Radiation on Porcine Vertebrae*. Dallas, Texas: Southern Methodist University.
- Reinwald, S., & Burr, D. (2008). Review of Nonprimate, Large Animal Models for Osteoporosis Research. *Journal of Bone and Mineral Research*, 23(9), 1353-1368.

- Renaud, G., Calle, S., Remenieras, J.-P., & Defontaine, M. (2008, July). Exploration of Trabecular Bone Nonlinear Elasticity Using Time-of-Flight Modulation. *IEEE Transactions on Ultrasonics, Ferroelectrics, and Frequency Control*, 55(7), 1497-1507.
- Rho, J. Y., Ashman, R. B., & Turner, C. H. (1993). Young's modulus of trabecular cortical bone material: Ultrasonic and microtensile measurements. *Journal of Biomechanics*, 26, 111-119.
- Richer, E., Lewis, M. A., Odvina, C. V., Vazquez, M. A., Smith, B. J., Peterson, R. D., et al. (2005). Reduction in normalized bone elasticity following long-term bisphosphonate treatment as measured by ultrasound critical angle reflectometry. *Osteoporosis International*, 16, 1384-1392.
- Rissanen, P., Rokkanen, P., & Paatsama, S. (1969). The effect of Co60 irradiation on bone in dogs. I. Mature bone. *Strahlentherapie*, 137(2), 162-169.
- Rissanen, P., Rokkanen, P., & Paatsama, S. (1969). The effect of Co60 irradiation of bone in dogs. II. Growing bone. *Strahlentherapie*, 137(3), 344-354.
- Rokkanen, P., Rissanen, P., & Paastama, S. (1969). The Effect of Co60 Irradiation on the Patella in Dogs. *Acta orthopaedica Scandinavica*, 40(5), 563-570.
- Rose, P. S., Laufer, I., Boland, P. J., Hanover, A., Bilsky, M. H., Yamada, J., et al. (2009). Risk of fracture after single fraction image-guided intensity-modulated radiation therapy to spinal metastases. *Journal of Clinical Oncology*, 27(30), 5075 - 5079.
- Smit, T. H. (2002). The use of quadruped as an invivo model for the study of the spine - biomechanical considerations. *European Spine Journal*, 11, 137-144.
- Smit, T. H., Odgaard, A., & Schneider, E. (1997). Structure and function of vertebral trabecular bone. *Spine*, 22, 2823-2833.
- Zhao, B., Basir, O., & Mittal, G. (2005). Estimation of ultrasound attenuation and dispersion using short time Fourier transform. *Ultrasonics*, 43(5), 375-381.
- Zimmermann, F. B., Geinitz, H., Schill, S., Grosu, A., Schratzenstaller, U., Molls, M., et al. (2005). Stereotactic hypofractionated radiation therapy for stage I non-small cell lung cancer. *Lung Cancer*, 48(1), 107-114.

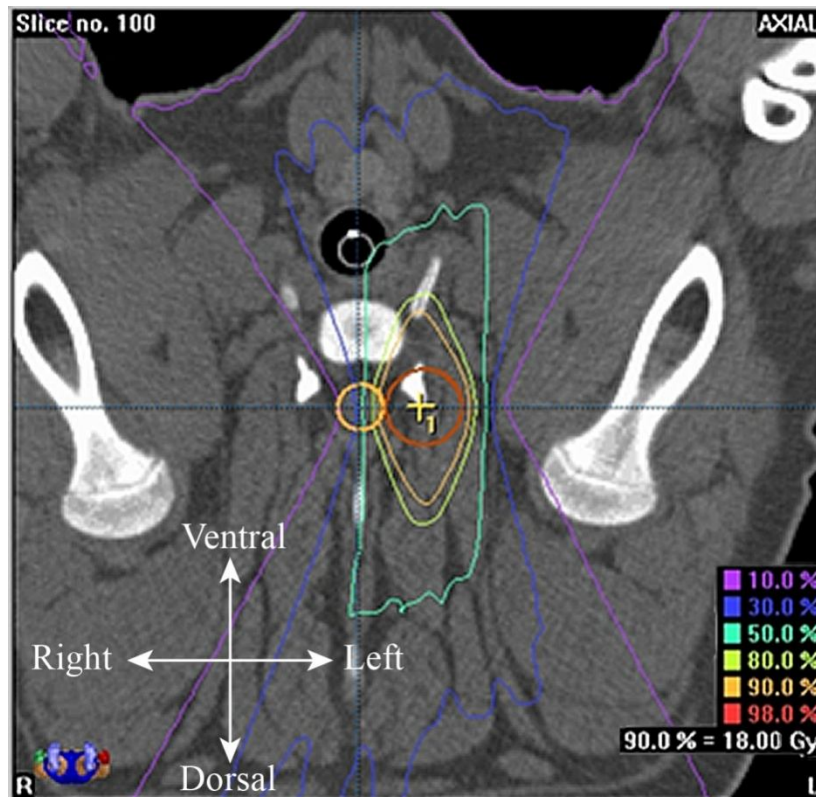


**Figure 1:** A rostral-caudal view of the radiation prescription plan from the fourth to the sixth cervical vertebra. The nominal dose distribution is shown by the green isoline. The targeted left side received 16 - 18 Gy while the right side received 6 - 8 Gy.

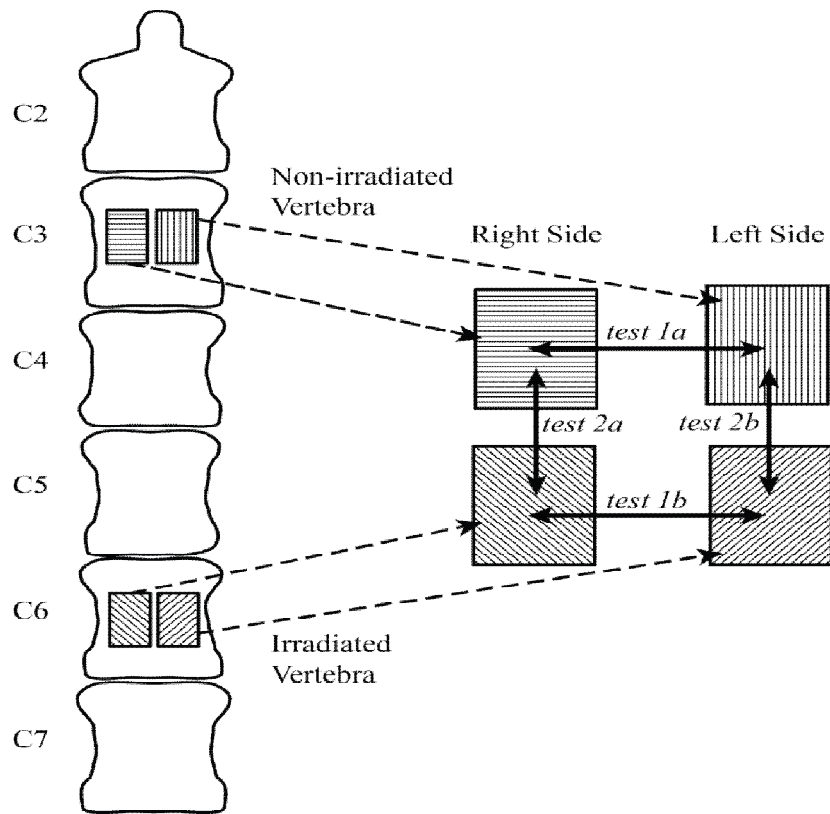


**Figure 2: Schematic of bone sample location of cervical vertebrae from C2 to C7. On the right, relationship of the bone samples for the four different *t*-tests conducted on the values for the UPV measurements are shown with the arrows.**

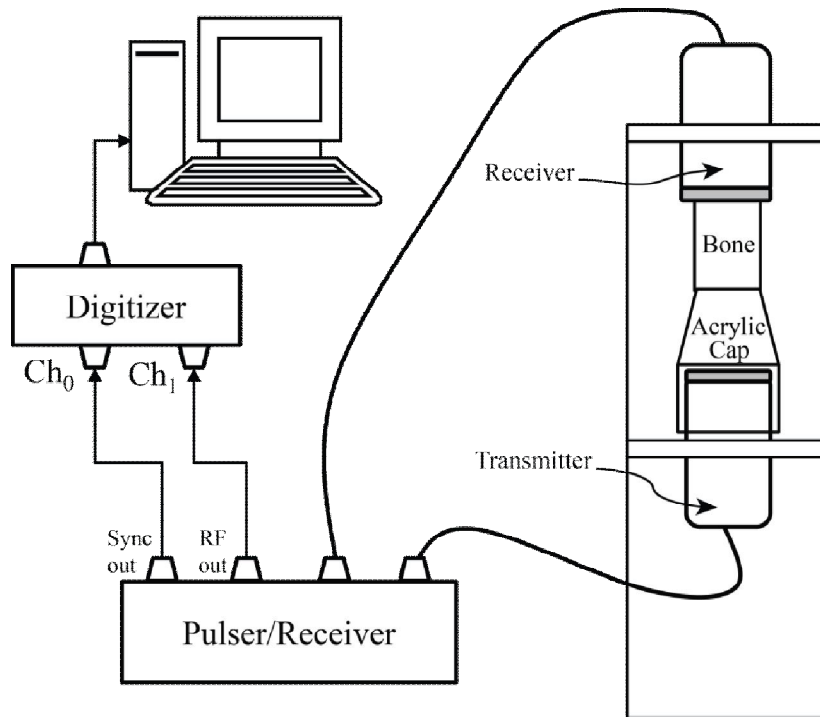


**Figure 3: Diagram of the experimental setup used for UPV and frequency measurements.**



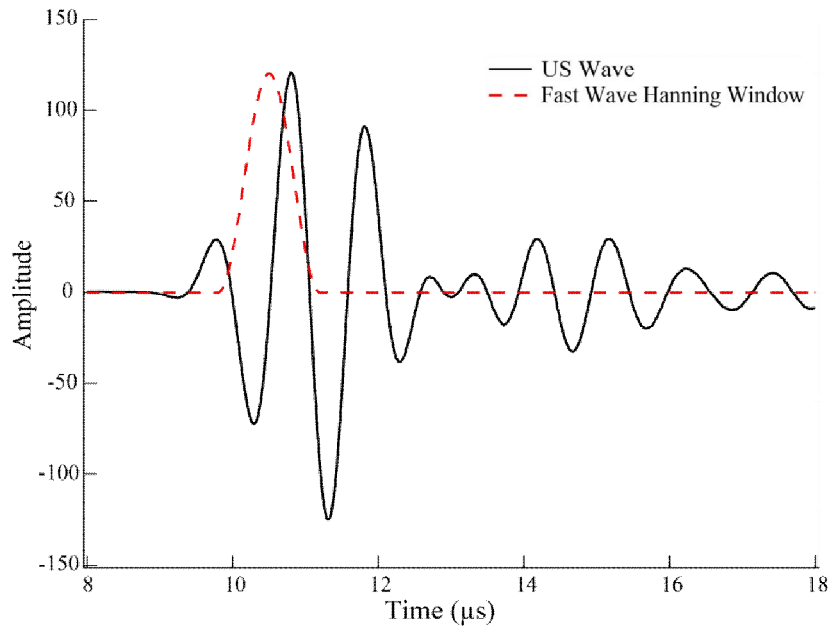


Figure 4: A typical ultrasound signal transmitted through trabecular bone samples (black, solid line). Red, dashed line shows the Hanning Window employed for the STFT.

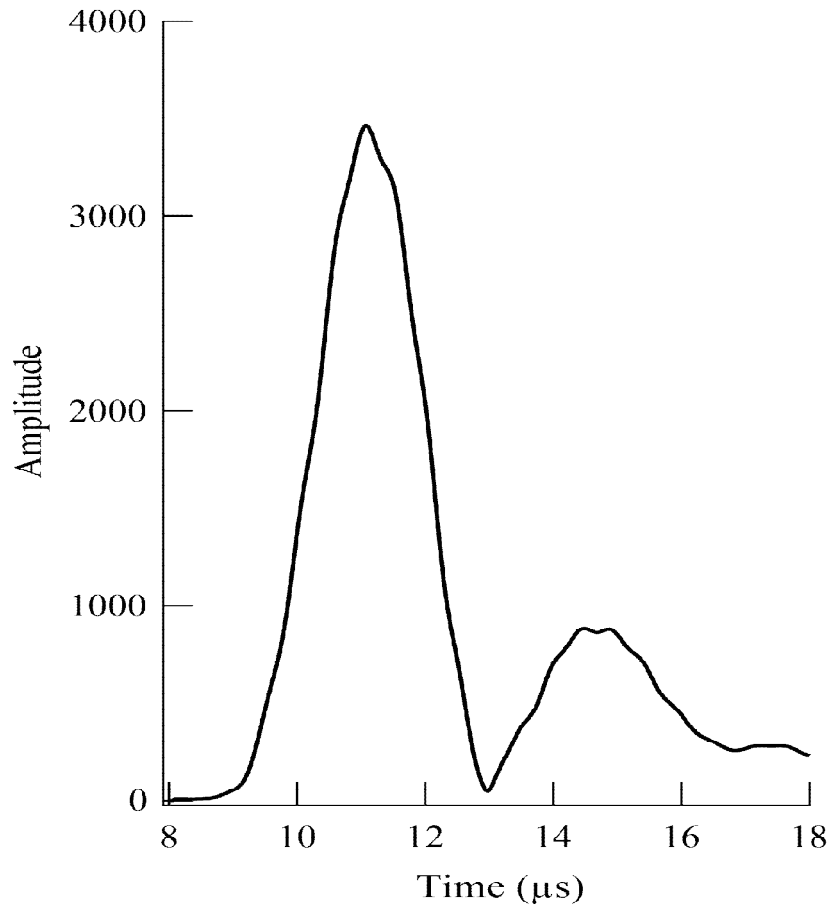
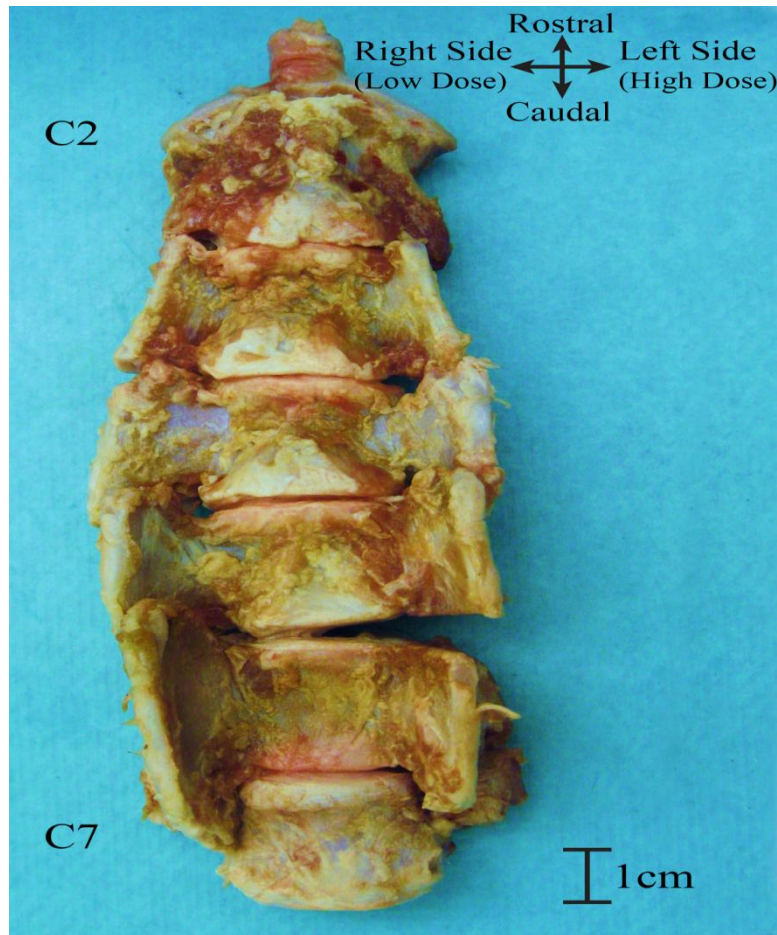
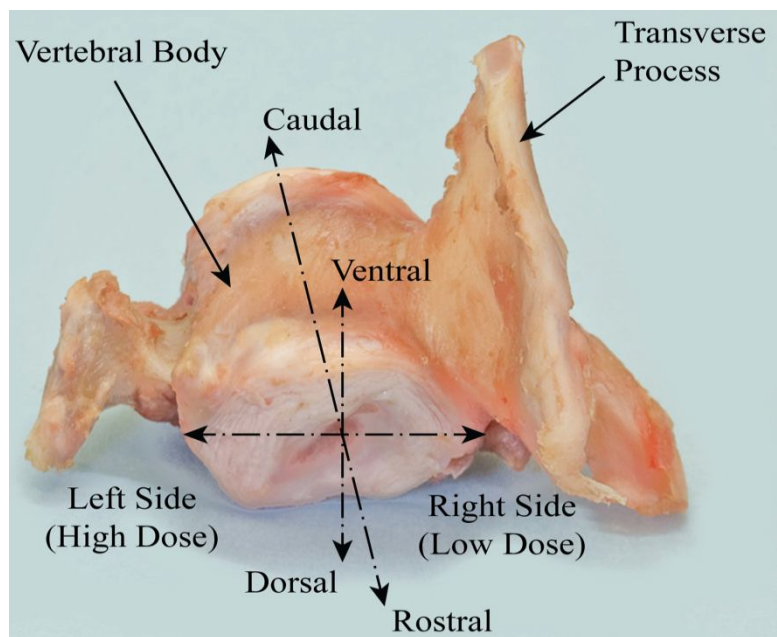


Figure 5: Frequency specific amplitude plot from STFT versus the moment of time,  $b$  in  $\mu s$ . The UPV was calculated using the moment of time ( $b$ ) of the location of the peak.



**Figure 6:** The ventral view of the cervical vertebrae of animal D from C2 to C7. Observable asymmetry between the high dose side and the low dose side for the irradiated vertebrae are apparent, in addition to the shorter length in the rostral/caudal direction.



**Figure 7:** The fifth vertebra of animal A, irradiated at 16 Gy on left half of the vertebral body. Besides vertebral body, shortening the left transverse process is completely atrophied.

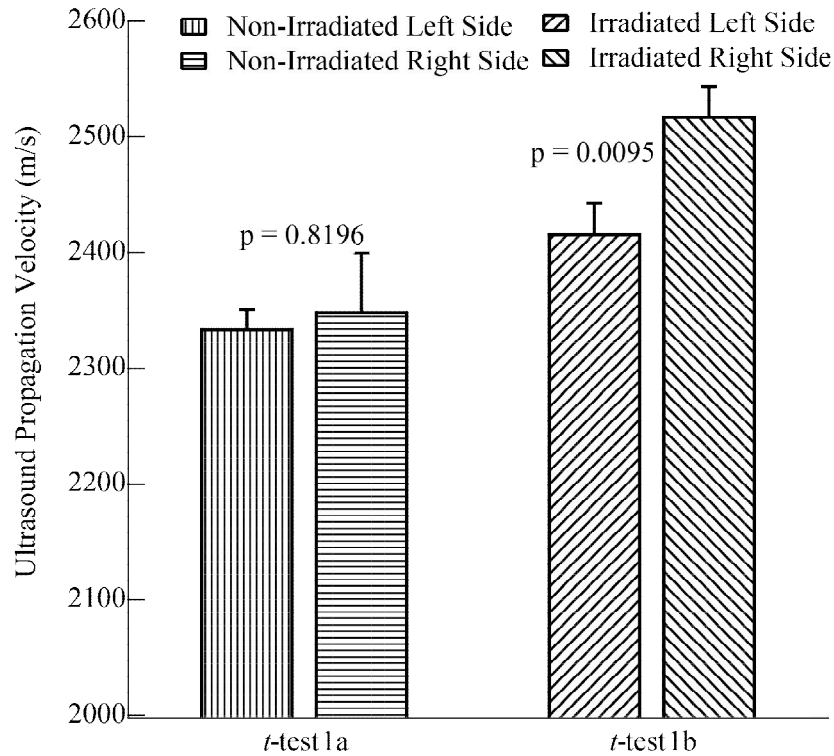


**Figure 8: Comparison of UPV for t-test 1. t-test 1a: compares the left side of the non-irradiated vertebra to the right side of the non-irradiated vertebra. t-test 1b: compares the left side of the irradiated vertebra to the right side of the irradiated vertebra.**

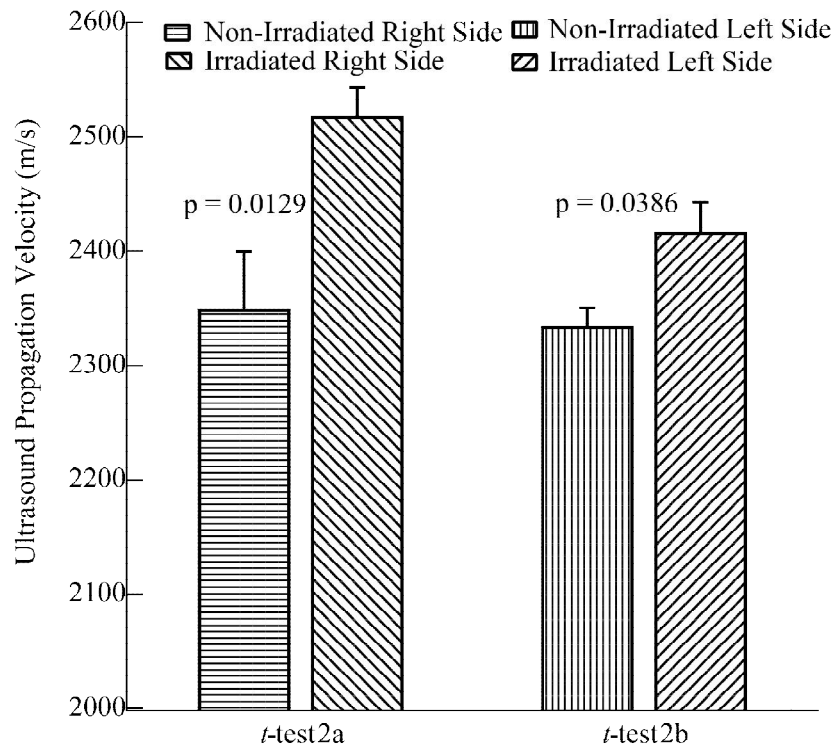


**Figure 9: Comparison of UPV for t-test 2. t-test 2a: Compares the Right Side of the Non-Irradiated Vertebra to the Right Side of the Irradiated vertebra. t-test 2b: Compares the Left Side of the Non-Irradiated Vertebra to the Left Side of the Irradiated Vertebra.**